J Fluoresc (2010) 20:37–41
DOI 10.1007/s10895-009-0519-2

ORIGINAL PAPER

Fluorescence Characterization of the Structural Heterogeneity of Polytene Chromosomes

Sunil K. Noothi · Mamata Kombrabail · Basuthkar J. Rao · G. Krishnamoorthy

Received: 20 April 2009 / Accepted: 8 July 2009 / Published online: 24 July 2009

Abstract Studies on the physical nature of the structural heterogeneity of chromatin in their native states are few. The eukaryotic chromatin as observed by dye staining studies is of heterogeneous intensity when observed by fluorescent stains, where less and more bright regions apparently correspond to euchromatin and heterochromatin respectively. These are also associated with differential gene expression where it is believed that euchromatin is transcriptionally more active due to increased flexibility. Unfixed squashed preparations of polytene chromosomes of *Drosophila* were stained with a dsDNA specific dye PicoGreen and fluorescence lifetimes as well as fluorescence anisotropy decay kinetics were measured. Here we report a positive correlation between fluorescence lifetimes and fluorescence intensities, and show that less bright regions corresponding to euchromatin have shorter lifetimes, whereas more bright regions corresponding to heterochromatin have longer lifetimes. We interpret this as less bright regions being more dynamic, a conclusion also supported by fluorescence anisotropy decay kinetics. We infer that the comparatively higher flexibility associated with euchromatin can be directly measured by fluorescence lifetimes and fluorescence anisotropy decay kinetics.

S. K. Noothi · B. J. Rao
Department of Biological Sciences,
Tata Institute of Fundamental Research,
Mumbai 400005, India

M. Kombrabail · G. Krishnamoorthy (✉)
Department of Chemical Sciences,
Tata Institute of Fundamental Research,
Homi Bhabha Road, Colaba,
Mumbai 400005, India
e-mail: gk@tifr.res.in

Keywords Heterochromatin · Euchromatin · Structural heterogeneity · Fluorescence lifetime · Fluorescence anisotropy · PicoGreen

Introduction

Eukaryotic chromatin can be broadly divided into euchromatin and heterochromatin based on the cytological appearance of fluorescence intensities when stained with extrinsic DNA specific dyes like Orcein, Carmine acetic acid etc. [1]. A considerable portion of the eukaryotic genome is represented by heterochromatin which is characterized by its bright cytological appearance throughout the cell cycle and is predominantly found at pericentromeric and telomeric chromosomal regions. This form of packaging of DNA in chromatin is attributed to result in gene silencing which in case of heterochromatin is also heritable [2]. Heterochromatin is rich in highly repetitive sequences in all species from *Drosophila* to *Arabidopsis* [3, 4]. The prevalence of repeats and the observation that long tandem arrays of some transgenes are associated with transcriptional silencing [5] suggests a mechanism wherein, pairing between the repeats leads to higher order structures with regular nucleosomal arrays [6]. Restricted accessibility to DNase I and restriction enzymes in heterochromatin, and position effect variegation (PEV- heritable silencing of gene expression resulting from translocation of the gene to a position close to heterochromatin) [7] are other indirect evidences for the rigidity of heterochromatin state leading to gene silencing.

Apart from the cytological and functional characterization of chromatin there is much less structural description of euchromatin and heterochromatin states although there have been attempts to estimate the flexibility of intact

chromosomes, wherein it was shown by steady state fluorescence anisotropy measurements that chromatin exhibits spatio temporal heterogeneity [8]. Although it is generally believed that euchromatin region is more flexible compared to heterochromatin region, to our knowledge, there does not seem to be any direct measurement on the comparative flexibility of these regions. The references (refs. 8, 9 and 18) cited by us also do not provide this information. It has also been reported that enzymatic disruption of histone tail-tail interactions leads to an increase in chromatin flexibility [9]. The fragmentation of DNA in apoptosis has also been detected with fluorescence lifetime measurements [11]. Fluorescence lifetime-based imaging techniques have also been used extensively and have provided a wealth of information. Fluorescence lifetime imaging of DNA has been done on fixed nuclei and the heterogeneity of lifetimes and spatial variation of FRET efficiency has been attributed to highly condensed regions of DNA [10]. However there was no distinct correlation between the state of chromatin based on lifetime and any other attribute. Also the sample used was fixed in this study. Although lifetime imaging methods would certainly provide more information in intact preparations where banding could be observed, a clear banding pattern is not possible without fixation of sample. Without a definite variable attribute with respect to the structure it would be difficult to make any correlation. Hence we have chosen the heterogeneous intensity pattern to correlate with the level of flexibility measured by fluorescence lifetime and fluorescence anisotropy decay kinetics. Fluorescence lifetime imaging does provide images based on lifetime variation as a contrast parameter. However the dynamic range in the imaging mode is generally inferior to that of single-point measurement carried out in the present work. A high dynamic range brings out small differences in fluorescence lifetime with enhanced reliability. Hence we chose single-point measurement method to establish correlations of this kind since we also expect that chromatin in its native state shows a continuum of dynamic changes in relation to its structure and function. Considering the importance of chromatin structure in controlling gene expression, information on the differences in the "physical state" of various regions of chromatin would be of immense use.

Experimental

Materials PicoGreen was obtained from Molecular Probes and the other chemicals were from Sigma Chemical Company.

Sample preparation A third instar larva of Drosophila Melanogaster was dissected and salivary glands were isolated as in ref (17). The glands were teased and incubated in 10 μl of PBS with a dilute solution of PicoGreen whose concentration was empirically determined and squashed gently. The slides were imaged and analyzed within a span of 2 h.

Time-resolved fluorescence microscope The set-up consists of three parts: (i) a picosecond laser system (ii) Fluorescence microscope and (iii) Time-Correlated-Single-Photon-Counting system. 914 nm pulses having FWHM of ~1 ps at a repetition rate of 4 MHz derived from a Ti-Sapphire (Spectra Physics, Palo Alto, USA) laser was steered into an epifluorescence microscope (Diaphot, Nikkon Corp., Japan) and focused to ~1 μm onto samples by using a 63X, NA 0.74 objective lens. The fluorescence collected by a dichroic filter (>470 nm) and a cut-off filter was passed through a polarizing beam splitter to get the emission in two channels with polarizations parallel and perpendicular to that of the excitation polarization which was fixed at vertical position. The emission was detected simultaneously by compact photon counting PMTs (Type H5773P-01 from Hammamatsu Corp., Japan) having instrument response functions with widths of ~160 ps. A photon counting card (SPC-630, Becker & Hickl, Germany) was used to perform timecorrelated- single-photon-counting with count rates in the range of $1–10\times10^4$ Hz. For fluorescence lifetime measurements, one of the emission polarisers was kept at the magic angle (54^0) and for anisotropy measurements, the emission was measured simultaneously at the two channels with parallel and perpendicular polarizations. The entire system was tested with several test samples for both lifetimes and rotational correlation times (see later).

Data analysis Time-resolved fluorescence intensity decay data (collected at the magic angle) were fitted to a function that is a sum of discrete exponentials,

$$I(t) = \sum \alpha_i \exp(-t/\tau_i)$$

where τ_i are fluorescence lifetimes and α_i are their amplitudes. $\sum\alpha_i=1$. Fitting was performed by the iterative deconvolution method. Fluorescence decay function of an oxonal derivative with a very short (<50 ps) lifetime was used as the instrument response function for the deconvolution. The width of the instrument response function was ~170 ps. The mean lifetime, $\tau_m=\sum\alpha_i\tau_i$, gives us information on the average fluorescence yield of the system.

In time-resolved fluorescence anisotropy measurements, the emission was collected at directions parallel ($I_\parallel$) and perpendicular ($I_\perp$) to the polarization of the excitation beam. The anisotropy was calculated

$$r(t) = \left[I_\parallel(t) - I_\perp(t)G(\lambda)\right] / \left[I_\parallel(t) + 2I_\perp(t)G(\lambda)\right]$$

where G(λ) is the geometry factor at the wavelength λ of emission. The geometry factor [G(λ)] of the emission collection optics was determined in separate experiments using a standard sample (fluorescein) for which the rotational correlation time was ~0.1 ns and fluorescence lifetime was ~4 ns. Time-resolved anisotropy decays were analyzed based on the following equation.

$$r(t) = r_0\{\beta_1 \exp(-t/\Phi_1) + \beta_2 \exp(-t/\Phi_2)\}$$

where r_0 is the initial anisotropy, β_i is the amplitude of the i^{th} rotational correlation time (Φi) such that $\Sigma\ \beta_i=1$. r_0 was estimated to be 0.33±0.01 from the anisotropy decay kinetics of PicoGreen in glycerol. The shorter component Φ_1, represents the internal motion of the probe and the longer correlation time Φ_2 represents a combination of segmental and global tumbling dynamics of the system.

The goodness of fits was evaluated by the value of reduced chi-square (1.0 to 1.2 as acceptable range) and the randomness of residuals.

Test of the time-resolved fluorescence microscope with standard samples The entire system was tested with several standard samples by measuring their lifetimes and rotational correlation times. The lifetimes and rotational correlation times for the standard samples were found to be as follows: *Fluorescein:* Lifetime: 4.1±0.2 ns and rotational correlation time: 90±30 ps. *Enhanced Green Fluorescent Protein (EGFP):* Lifetimes: 2.8±0.2 ns (66 %) and 1.3 ±0.1 ns (34 %) and rotational correlation time: 10.3±0.8 ns.

Results and discussion

In this work, we show evidence substantiating the prevalent idea of the physical state of eukaryotic chromatin, that euchromatin is more flexible than heterochromatin. We report a correlation between the cytological appearance of unfixed squashed polytene chromosomes of *Drosophila* salivary glands and its local flexibility by measuring the variations in the fluorescence lifetime of an extrinsic DNA specific dye called PicoGreen (PG). PG, an unsymmetric monomethine cyanine dye [12, 13] has found interesting applications in scoring the level of nicks and cuts in DNA [14] presumably through changes in the rate of nonradiative decay process controlled by internal rotation of DNA-bound dye. The fluorescence quantum yield of PG and other DNA-binding dyes such as YOYO is predominantly controlled by molecular rotation-aided internal conversion and hence it acts as a reporter of DNA flexibility [15, 16].

In this study, we have measured fluorescence lifetimes of PicoGreen-stained unfixed polytene chromosomes of Drosophila salivary glands in a spatially resolved manner under a fluorescence microscope [17]. Fixation was avoided in these preparations at the expense of a banding pattern so that the measured lifetimes could reflect the native environment around chromatin. Figure 1 shows an example of a squashed preparation without fixation where regions of varying brightness can be seen. It should be noted that classical banding patterns cannot be obtained with such unfixed preparations. However, it is very likely that the regions of varying brightness seen in these preparations correspond to the banding pattern obtained with a variety of DNA stains, with the less and more bright regions corresponding to euchromatin and heterochromatin states respectively. Fluorescence lifetimes were measured at different positions corresponding to varying brightness levels. Fluorescence lifetime is an ideal parameter to estimate changes in the level of non-radiative processes (controlled by internal motion of DNA-bound PicoGreen) as opposed to fluorescence intensity, as the latter is also controlled by factors such as sample geometry, collection efficiency etc.

Figure 2 is a plot of several such measurements of fluorescence lifetimes against integrated fluorescence intensity measured at various locations. An intensity decay of two representative positions of less and more bright intensities is shown in inset of Fig. 2. It can be seen that the variation in the fluorescence intensity (brightness) is ~3 fold and more importantly, there is a clear correlation between the fluorescence lifetime and the intensity. Low intense regions correspond to shorter lifetimes and regions of higher brightness are associated with longer lifetimes. When we recall that shortening of fluorescence lifetime of PG is mainly caused by internal motion-caused non-radiative decay, we get a picture that low intense regions

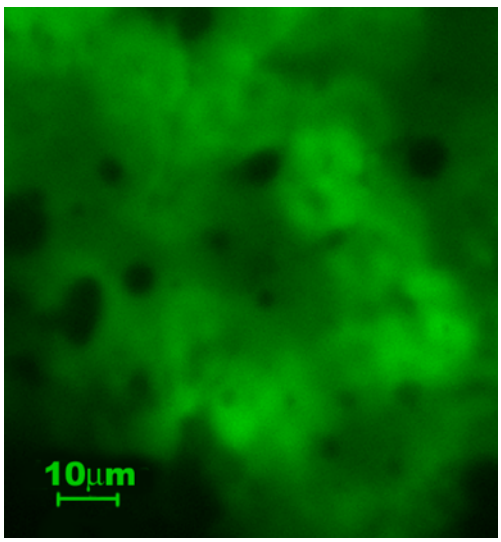

Fig. 1 Fluorescence microscopy image of squashed polytene chromosome stained with PicoGreen

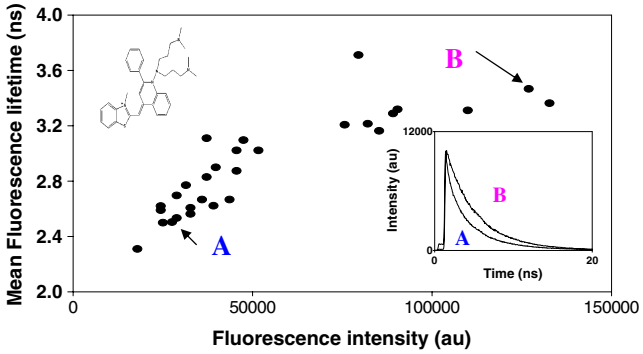

Fig. 2 Plot of mean fluorescence lifetimes against integrated fluorescence intensity. Fluorescence intensity decay of two representative regions of less and more bright intensities (marked *A* and *B*) are shown in inset. Inset on the left shows the structure of PicoGreen. Fluorescence decay curves were analyzed as a sum of three exponentials. $I(t)=\Sigma_i\ \alpha_i\ \exp\ (-t/\tau_i)$, I=1-3, where αi are the amplitudes and τi are the fluorescence lifetimes. $\Sigma_i\ \alpha_i=1$. Mean lifetime, $\tau_m=\Sigma_i\ \alpha_i\ \tau_i$. For more details see "Experimental" Section and ref [19]

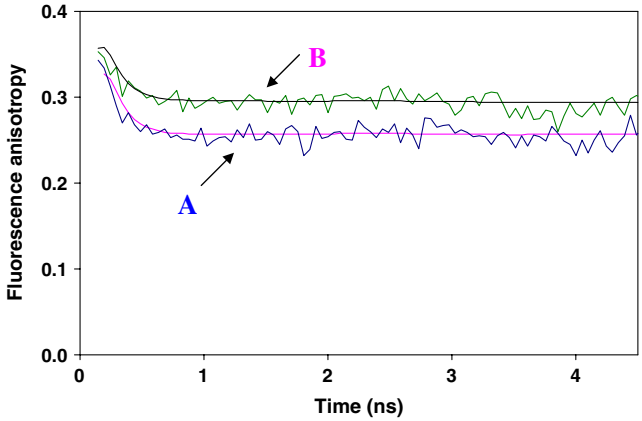

Fig. 3 Fluorescence anisotropy decay kinetics of representative less (*A*) and more (*B*) bright regions of polytene chromosomes. The anisotropy (r) decay kinetics was analyzed as a sum of two exponentials representing fast and slow rotational correlation times [19]. $r(t) = r0\left[\beta_1 \exp\left(-t/\varphi_1\right) + \beta_2 \exp\left(-t/\varphi_2\right)\right]$, where r0 (0.33) is the initial anisotropy, ϕ is the rotational correlation time and β is the amplitude, $(\beta_1 + \beta_2 = 1)$. The values of β_1 (amplitude of the faster motion) are 0.26±0.02 and 0.14±0.02 for the less and more bright regions respectively, marked *A* and *B* as in Fig. 2. The values of φ_1 and φ_2 are 80±40 ps and >100 ns respectively for both the traces. Smooth lines represent the fits to the data

(euchromatin) are associated with higher level of flexibility when compared to brighter (heterochromatin) regions. We point out that the observed positive correlation between fluorescence intensity and lifetime is unlikely to arise from the trivial relationship between quantum yield and fluorescence lifetime. Fluorescence intensity is proportional to the quantum yield and the concentration of the fluorphore and quantum yield is proportional to fluorescence lifetime. Hence fluorescence intensity will be proportional to lifetime only when the concentration of the fluorophore remains constant. Since the concentration of fluorophore is not expected to be the same at all the locations in the sample, we do not expect the observed positive correlation between the intensity and lifetime to arise from the above relationships. Hence, the observed correlation has to have its origin on a combination of position-dependent changes in quantum yield and changes in concentration of the fluorophore.

Variation in the level of flexibility inferred from changes in the fluorescence lifetime of PG (Fig. 2) was also supported by direct observation of motional dynamics extracted from time-resolved fluorescence anisotropy decay kinetics. Decay profiles obtained from representative high and low intensity regions (Fig. 3) show that the amplitude (β_1) associated with the faster (~80 ps) component of decay kinetics is higher (0.26±0.02) in the low brightness region (trace A) when compared to the high brightness region (0.14±0.02, trace B). The observed 80 ps rotational correlation time is not possible to come from free PicoGreen in solution as its quantum yield in aqueous buffer is very low and well beyond our detection limit. Furthermore, any presence of aqueous PG would have resulted in a 'dip-and-rise' anisotropy decay kinetics which is a hallmark of the presence of two populations. The dip-and-rise anisotropy decay kinetics pattern was not observed at any of the locations probed. In fact, very short rotational correlation times (~100 ps) of fluorescence probes bound, either covalently or non-covalently, to DNA have been attributed to flexibility of the macromolecule.

When we recognize that changes in β_1 reflect changes in the level of internal motion of the fluorophore arising from changes in the flexibility of the macromolecule [15, 19] we get a picture that the flexibility is higher in locations of low brightness when compared to regions of higher brightness. Very often, changes in the level of flexibility in macromolecules is reflected in changes in the amplitude associated with the internal motion rather than in the rate of internal motion [15, 19] as observed in the present situation. The longer correlation time (>100 ns, limited by the time window offered by the fluorescence lifetime) is due to restriction in the motional dynamics of bound PG. Absence of observable changes in the longer correlation time is likely to be due to the limited time window due to the small lifetime of the probe (~4.5 ns for PicoGreen).

The interpretation of our results is quite straight forward. Euchromatin regions are more flexible when compared to heterochromatin regions. The higher flexibility of euchromatin would have endowed a higher degree of internal motion of DNA-bound PicoGreen. Such a model would also confer heterochromatin as a highly condensed form when compared to euchromatin. The functional implication of this interpretation is also clear. The higher level of

dynamics associated with euchromatin could be the cause of it's flexibility, which allows euchromatin to be amenable for transcription. The necessity of interaction of protein factors in transcription would also require the DNA to be in a relatively more flexible and accessible state.

We believe that our results offer the first and direct information on the comparative flexibility of the well documented higher order structures in eukaryotic chromatin in its native state unprocessed by extraneous treatments. A recent comparative study on the mechanical properties of euchromatin and heterochromatin suggested a role for heterochromatin in imparting mechanical stability of the cell nucleus [18]. The Drosophila polytene chromosome in conjunction with the facile genetics that this model system offers, would enable a direct physical analyses (as described in the current study) between chromatin remodeling/compaction and the molecular mechanisms that are causally related to their functions. Having shown the "proof of the concept" experiment here, our future efforts would focus on using the analyses in different genetic backgrounds that affect chromatin dynamics and biological function.

Acknowledgements We thank Dr. Anoop Saxena and Swagata Chakraborthy for their help in experiments with TCSPC-microscope and Prof. N. Periasamy for software used in the analysis of fluorescence decay kinetics.

References

1. Heitz E (1928) Das heterochromatin der moose. I Jahrb Wiss Botanik 69:762–818
2. Dillon N, Festenstein R (2002) Unravelling heterochromatin: competition between positive and negative factors regulates accessibility. Trends Genet 18:252–258
3. Smith CD, Shu S, Mungall CJ, Karpen GH (2007) The Release 5.1 annotation of Drosophila melanogaster heterochromatin. Science 316:1586–1591
4. Biosystems Arabidopsis Sequencing Consortium (2000) Cell 100:377–386
5. Henikoff S (1998) Conspiracy of silence among repeated transgenes. Bioessays 20:532–535
6. Sun FL, Cuaycong MH, Elgin SC (2001) Long-range nucleosome ordering is associated with gene silencing in Drosophila melanogaster pericentric heterochromatin. Mol Cell Biol 21:2867–2879
7. Schotta G, Ebert A, Dorn R, Reuter G (2003) Position-effect variegation and the genetic dissection of chromatin regulation in Drosophila. Semin Cell Dev Biol 14:67–75
8. Banerjee B, Bhattacharya D, Shivashankar GV (2006) Chromatin structure exhibits spatio-temporal heterogeneity within the cell nucleus. Biophys J 91:2297–2303
9. Roopa T, Shivashankar GV (2006) Direct measurement of local chromatin fluidity using optical trap modulation force spectroscopy. Biophys J 91:4632–4637
10. Murata S, Herman P, Lin HJ, Lakowicz JR (2000) Fluorescence lifetime imaging of nuclear DNA: effect of fluorescence resonance energy transfer. Cytometry 41:178–185
11. Sailer BL, Valdez JG, Steinkamp JA, Crissman HA (1998) Apoptosis induced with different cycle-perturbing agents produces differential changes in the fluorescence lifetime of DNA bound ethidium bromide. Cytometry 31:208–216
12. Zipper H, Brunner H, Bernhagen J, Vitzthum F (2004) Investigations on DNA intercalation and surface binding by SYBR Green I, its structure determination and methodological implications. Nucleic Acids Res 32:e103
13. Singer VL, Jones LJ, Yue ST, Haugland RP (1997) Characterization of PicoGreen reagent and development of a fluorescence-based solution assay for double-stranded DNA quantitation. Anal Biochem 249:228–238
14. Cosa G, Vinette AL, McLean JR, Scaiano JC (2002) DNA damage detection technique applying time-resolved fluorescence measurements. Anal Chem 74:6163–6169
15. Nag N, Ramreddy T, Kombrabail M, Krishna Mohan PM, D'souza J, Rao BJ, Duportail G, Mely Y, Krishnamoorthy G (2006) Dynamics of DNA and Protein-DNA complexes viewed through time-domain fluorescence. In: Geddes CD, Lakowicz JR (eds) Reviews in Fluorescence, vol 3. Springer, US, pp 311–340
16. Cosa G, Focsaneanu K-S, Scaiano JC, McLean JRN (2000) Direct determination of single-to-double stranded DNA ratio in solution applying time-resolved fluorescence measurements of dye-DNA complexes. Chem Commun 689–690
17. Pardue ML (1994) Looking at polytene chromosomes. Methods Cell Biol 44:333–351
18. Mazumder A, Shivashankar GV (2007) Gold-nanoparticleassisted laser perturbation of chromatin assembly reveals unusual aspects of nuclear architecture within living cells. Biophys J 93:2209–2216
19. Nag N, Rao BJ, Krishnamoorthy G (2007) Altered dynamics of DNA bases adjacent to a mismatch: a cue for mismatch recognition by MutS. J Mol Biol 374:39–53